Increased CD8+ T-cell Function following Castration and Immunization Is Countered by Parallel Expansion of Regulatory T Cells

Shuai Tang[1,4], **Miranda L. Moore**[1], **Jason M. Grayson**[3], and **Purnima Dubey**[1,2,3,4,5]

[1]Department of Pathology-Tumor Biology, Wake Forest School of Medicine, Winston-Salem, North Carolina

[2]Department of Cancer Biology, Wake Forest School of Medicine, Winston-Salem, North Carolina

[3]Department of Microbiology & Immunology, Wake Forest School of Medicine, Winston-Salem, North Carolina

[4]Department of Molecular Pathology Graduate Program, Wake Forest School of Medicine, Winston-Salem, North Carolina

[5]Comprehensive Cancer Center, Wake Forest School of Medicine, Winston-Salem, North Carolina

Abstract

Although androgen ablation therapy is effective in treating primary prostate cancers, a significant number of patients develop incurable castration-resistant disease. Recent studies have suggested a potential synergy between vaccination and androgen ablation, yet the enhanced T-cell function is transient. Using a defined tumor antigen model, UV-8101-RE, we found that concomitant castration significantly increased the frequency and function of antigen-specific CD8+ T cells early after the immunization of wild-type mice. However, at a late time point after immunization, effector function was reduced to the same level as noncastrated mice and was accompanied by a concomitant amplification in CD4+CD25+Foxp3+ regulatory T cells (Treg) following immunization. We investigated whether Treg expansion occurred following castration of prostate tumor–bearing mice. In the prostate-specific *Pten*$^{-/-}$ mouse model of prostate cancer, we observed an accelerated Treg expansion in mice bearing the castration-resistant endogenous prostate tumor, which prevented effector responses to UV-8101-RE. Treg depletion together with castration elicited a strong CD8+ T-cell response to UV-8101-RE in *Pten*$^{-/-}$ mice and rescued effector function in castrated and immunized wild-type mice. In addition, Treg expansion in *Pten*$^{-/-}$ mice was prevented by *in vivo* interleukin (IL)-2 blockade suggesting that increased IL-2 generated by castration and immunization promotes Treg expansion. Our findings therefore suggest that although effector responses are augmented by castration, the concomitant expansion of Tregs is one mechanism responsible for only transient immune potentiation after androgen ablation.

Corresponding Author: Purnima Dubey, Wake Forest School of Medicine, 2104 Gray Building, Medical Center Blvd. Winston-Salem, NC 27157. Phone: 336-716-7078; Fax: 336-716-6757; pdubey@wakehealth.edu.

Note: Supplementary data for this article are available at Cancer Research Online (http://cancerres.aacrjournals.org/).

Disclosure of Potential Conflicts of Interest
No potential conflicts of interests were disclosed.

Introduction

Prostate cancer is the most commonly diagnosed malignancy and the second leading cause of cancer-related deaths in males of the Western world (1). Effective treatment of prostate cancer currently involves radical prostatectomy, radiation therapy, and/or androgen ablation (2). Removal of androgen leads to decreased proliferation and programmed cell death in prostate epithelial cells. Castration-resistant tumor and metastatic disease that may arise years later is largely incurable.

Immune therapy may be a promising treatment modality for castration-resistant prostate cancer (3). However, the role of androgen in modulating immune function and the consequence of androgen removal/blockade on adaptive immune responses is not completely understood. Androgen is generally considered as immunosuppressive, and hormone removal increases T-cell function in autoimmune disease models (4, 5). These observations suggest that androgen removal may augment T-cell responses following immunization against prostate tumor antigens, including self-proteins. However, CD8^{+} T-cell responses to a prostate self-antigen expressed in murine prostate cancer cells were only accentuated if immunization was before castration (6). In contrast, the function of transgenic CD8^{+} T-cells specific for prostate-specific antigen was enhanced until 4 weeks after castration (7). Furthermore, in a CD4^{+} transgenic T-cell model, a synergy between androgen deprivation and vaccination alleviated systemic tolerance to a model prostate tumor antigen and increased T-cell proliferation early after castration (8). Thus, the ability of androgen ablation to augment immune responses to prostate tumor antigens may depend on the antigen in question and the strength of the T-cell response.

To determine the mechanism responsible for transiently increased effector function, we first investigated the effect of androgen ablation on CTL responses to a well-defined immunodominant tumor antigen in nontumor-bearing C57BL/6 mice. The ultraviolet light–induced murine sarcoma, UV-8101-RE, expresses a mutant tumor-specific protein that induces a strong CD8^{+} T-cell response (9). We immunized mice intraprostatically with this antigen and found that concomitant castration enhanced the proportion of antigen-specific CD8^{+} T cells in the spleen and increased their function early after immunization, which declined by 5 weeks after immunization. However, we also observed an increased proportion of CD4^{+}CD25^{+}Foxp3^{+} regulatory T cells (Tregs) in the castrated and immunized animals.

We previously showed that functional CD8^{+} T cells responding to unknown prostate tumor antigens transiently increased following castration of prostate-specific $Pten^{-/-}$ mice (10). In this study, we show that castration of $Pten^{-/-}$ mice also expanded Tregs. An increased frequency of functional CD8^{+} T cells was only detected when Tregs were depleted before castration and immunization with the model antigen UV-8101-RE. We further show that in $vivo$ blockade of interleukin (IL)-2 prevents Treg expansion. Thus, androgen ablation amplifies both stimulatory and inhibitory arms of the immune system.

Materials and Methods

Animals and cell lines

C57BL/6 mice (8- to 12-week-old; Jackson Laboratory) were maintained under pathogen-free conditions in accordance with Institutional Animal Care and Use Committee guidelines. Prostate-specific $Pten^{-/-}$ mice (12- to 16-week-old) on the syngeneic C57BL/6 background were bred as described previously (10, 11). UV-8101-RE (from Dr. Hans Schreiber, University of Chicago, Chicago, IL) and TRAMP-C1 (from Dr. Owen Witte, UCLA, Los Angeles, California) cell lines were cultured as described previously (10). The authenticity

of UV-8101-RE was determined by specific killing of the cell line by α-8101–specific T cells that also recognize the mutant peptide epitope. Expression of SV40 viral DNA sequences and H-2K^b were determined in TRAMP-C1 cells.

Surgery

Mice were injected intraperitoneally (i.p.) with ketamine and xylazine (23.75 mg/mL ketamine + 1.25 mg/mL xylazine; 150 mg/kg). A lower midline incision was made and testes were removed. For immunization, 1×10^6 live UV-8101-RE cells in 20 μL volume, containing bromphenol blue for visualization were injected into both anterior and dorsal lobes of the prostate. All surgical and postsurgical care was in accordance with Wake Forest School of Medicine (WFSM) Winston-Salem, NC, Animal Care and Use Committee guidelines.

ELISPOT assays

Rat anti-mouse IFN-γ antibody (2.5 μg/mL, clone R4-6A2; BD Pharmingen) was used to coat 96-well filtration plates (Millipore). Splenocytes (1×10^6) were stimulated *ex vivo* with UV-8101-RE cells at 1:1 ratio with irradiated (1,200 rad) syngenic splenocytes as feeder cells for 36 hours in RPMI-1640 medium supplemented with 10% fetal calf serum, 4 mmol/L L-glutamine, and 50 μmol/L 2-mercaptoethanol. After culture, plates were washed and incubated with biotinylated anti-IFN-γ antibody (2.5 μg/mL, clone XMG 1.2; BD Pharmingen). Spots were developed with 3,3′-diaminobenzidine (DAB) substrate (Sigma). The plates were scanned with a plate scanner (Cellular Technology Ltd.) equipped with Image Acquisition 4.5 software, counted using ImageJ software (www.rsbweb.nih.gov/ij) and calculated as number of spot-forming cells per spleen.

Mixed lymphocyte tumor cell cultures and ^{51}Cr release assays

Mixed lymphocyte tumor cell cultures (MLTC) and ^{51}Cr release assays were conducted as described previously (9). The percentage of specific lysis was calculated by the formula: % cytolysis = [(experimental release – spontaneous release)/(maximum release – spontaneous release)] × 100.

Treg depletion

Tregs were depleted by a single i.p. injection of 0.5 mg anti-CD25 antibody (ref. 12; clone PC61; BioXCell), 2 days before castration and/or immunization.

IL-2 neutralization

To neutralize IL-2 function, mice were given 1 mg of anti-IL-2 mAb (clone S4B6; BioXCell) or isotype control i.p. 2 days before castration or sham surgery, as previously described (13).

Peptide production

The mutant p68 RNA helicase peptide (SNFVFAGI) was produced by the WFSM Protein Analysis Core Laboratory essentially as described previously (9). Briefly, the peptide was synthesized on an Applied Biosystems Model 430B automated peptide synthesizer, using the standard Applied Biosystems FastMoc solid-phase peptide synthesis chemistry protocol. The peptide identity and purity were shown by reverse-phase high-performance liquid chromatography, quantitative amino acid analysis, and matrix-assisted laser desorption/ionization—time-of-flight (MALDI-TOF) mass spectrometry.

Flow cytometric analysis

Splenocytes were dissociated and stained with fluorochrome-conjugated antibodies specific for CD4 [clone RM4-5, fluorescein isothiocyanate (FITC)-conjugated], CD8 (clone 53-6.7, FITC-conjugated), and CD62L [clone MEL-14, allophy-cocyanin (APC)-conjugated] from BD Pharmingen; and CD44 [clone IM7, phycoerythrin (PE)-conjugated] and CD25 (clone PC61.5, PE-conjugated) from eBioscience, all used at 1:100 dilution. Tregs were analyzed using the mouse Treg Staining Kit (eBioscience), and manufacturer's instructions. Cells were analyzed on a FACSCalibur equipped with Cellquest PRO software (BD Biosciences).

Tetramer production

MHC monomer was constructed and purified as described (14), except a plasmid clone expressing H-2K^b was used. The folding, purification, and biotinylation of K^b + peptide complexes were conducted as described (15). To prepare tetramer, 20 μL of monomer (2 mg/mL) was incubated at room temperature with one tenth volume of 128 μL streptavidin-PE (0.5 mg/mL; Jackson ImmunoResearch) or 95 μL streptavidin-PerCP-Cy5.5 (0.2 mg/mL; BD Pharmingen) added in 10-minute intervals and incubated in the dark.

Tetramer enrichment

Tetramer enrichment was conducted as described previously (16). Dissociated splenocytes stained with PE- and PerCP-Cy5.5–conjugated tetramers (4 μg/mL each) were also co-stained with CD8-FITC and CD44-APC. PE tetramer–positive cells were enriched with anti-PE magnetic beads (BD Biosciences) and analyzed on a FACSCalibur. Tetramer-positive cells were defined as PE and PerCP-Cy5.5 double-positive cells when gated on the CD8$^+$CD44$^+$ population. Nearly 100% of the tetramer-positive cells were CD44^{hi}.

Intracellular cytokine staining

MLTC cell suspensions were restimulated with UV-8101-RE cells at the ratio of 1:1 for 4 hours in the presence of 10 μg/mL brefeldin A (Sigma). TRAMP-C1 cells were used as negative control. Following surface CD8 staining, intracellular staining for IFN-γ (cloneXMG1.2; BDPharmingen) was conducted with the Cytofix/Cytoperm Kit (BD Biosciences).

TGF-β ELISA

Blood samples were collected from mice by cardiac puncture and the serum harvested by centrifugation. Total TGF-β levels were determined using a commercial ELISA kit (Promega).

Statistical analysis

Statistical comparisons were conducted using the unpaired Student t test with a 2-sided α level of 0.05. Differences in values at $P < 0.05$ were considered significant.

Results

Precursor frequency and function of CD8$^+$ T cells responding to a model tumor antigen increased following castration and immunization of nontumor-bearing mice

Previous studies reported that castration induces infiltration of T cells into the prostate in both normal (17) and prostate tumor–bearing mice (10, 17). Using the prostate-specific *Pten*$^{-/-}$ mouse model of endogenous prostate cancer, we showed that the accumulation of functional T cells in the prostate glands is not long-lasting, evident at 2.5 weeks after castration but diminished at 5 weeks after castration (10).

Antigens shed by dying prostate cancer cells after castration may stimulate $CD8^+$ T-cell responses. In an effort to track effector responses to an antigen located in the prostate, we used a defined tumor model system. The C57BL/6-derived murine sarcoma cell line UV-8101-RE expresses an $H-2K^b$–restricted immunodominant antigen, which elicits a strong CTL response that rejects the tumor cells (9). To model T-cell interactions to prostate antigens, normal male C57BL/6 mice were immunized with UV-8101-RE cells intraprostatically in both anterior and dorsolateral prostate lobes and were either castrated or sham-treated. Spleens and prostate draining lymph nodes (PDLN) were harvested 2.5 weeks later.

To quantify the number of UV-8101–specific responding $CD8^+$ T cells, we produced $H-2K^b$ tetramers complexed with the mutant peptide. Primary *ex vivo* analysis of splenocytes detected an increased frequency of tetramer-positive $CD8^+$ T cells in castrated and immunized mice, compared with sham-castrated mice (Fig. 1A). ELISPOT analysis also detected increased IFN-γ–secreting cells in the PDLNs and spleens (Fig. 1B), confirmed by *in vitro* analysis of cultured splenocytes (Fig. 1C and D). Thus, castration increased the number and functional capacity of $CD8^+$ T cells specific for UV-8101-RE.

Enhanced effector function declined 5 weeks after castration and immunization of nontumor-bearing mice

To determine the longevity of effector responses after castration and immunization, we evaluated mice 5 weeks following treatment. The frequency of tetramer-positive cells was similar in castrated or sham-castrated mice (Fig. 2A). Both groups also had similar numbers of IFN-γ–secreting cells in the spleens or PDLNs as determined by ELISPOT analysis (Fig. 2B). MLTCs from mice that were castrated or sham-castrated had low lytic activity (Fig. 2C) and IFN-γ production (Fig. 2D) after *ex vivo* restimulation at 5 weeks after treatment. Thus, increased function after castration diminished rapidly.

Castration increased splenic Tregs following immunization of nontumor-bearing mice

We investigated the mechanism for transient effector function after castration. Systemic Tregs can suppress $CD8^+$ T-cell responses to immunization (18-20). We quantified the proportion and number of Tregs in wild-type animals following immunization and found similar levels at 2.5 weeks following castration and immunization, compared with sham-castrated and immunized mice (Fig. 3A). Interestingly, we detected a modest but significant increase in the percentage of Tregs 5 weeks after castration and immunization (Fig. 3B, representative flow dot plots in Supplementary Fig. S1). The numbers of Tregs were also increased because the spleens were larger after castration (data not shown) as previously reported (5, 21). The frequency and number of Tregs in PDLNs was similar in castrated and intact immunized mice (data not shown). In addition, Tregs expanded only after immunization, as castration alone did not increase Treg proportion or number in the spleen at either time point (Fig. 3C) or in the PDLNs (data not shown), which is consistent with previous reports (5, 22).

If immunization was done 5 weeks after castration, lytic capacity (Supplementary Fig. S2A) and effector cytokine production (Supplementary Fig. S2B) of MLTC cells were not enhanced. Thus, reduced $CD8^+$ effector function at 5 weeks after castration may be due to inhibition by increased Tregs.

Castration expanded Tregs in prostate-specific *Pten*$^{−/−}$ mice

We previously reported that functional granzyme B^+CD8^+ T cells were increased in cancerous glands of prostate-specific *Pten*$^{−/−}$ mice 2.5 weeks after castration and declined by 5 weeks after castration (10). To determine whether increased Tregs accounted for this

decline, we measured systemic Treg levels in $Pten^{-/-}$ mice. The number of Tregs was significantly increased in PDLNs (Fig. 4A, top), and the number and frequency of Tregs increased in the spleen of castrated $Pten^{-/-}$ mice 2.5 weeks after castration compared with intact or sham-treated mice (Fig. 4A, bottom). Treg numbers remained elevated in the spleens of $Pten^{-/-}$ mice 5 weeks after castration (Fig. 4B, bottom). These data show that Treg expansion is induced by castration in tumor-bearing mice and may downregulate the function of CD8^{+} T cells activated after castration (10).

CD8^{+} T-cell effector responses against UV-8101-RE were generated only with concomitant castration and Treg depletion of $Pten^{-/-}$ mice

To determine whether the increased Tregs would prevent generation of effector function to a defined tumor antigen, we castrated and immunized $Pten^{-/-}$ mice intraprostatically with UV-8101-RE cells. A similar number of tetramer-positive cells was detected in the spleens of castrated or sham-treated mice 2.5 weeks after treatment (Fig. 5A), suggesting that castration did not increase the number of responding cells. Tetramer analysis was not conducted on lymph nodes due to insufficient numbers of cells for analysis of individual mice. In addition, ELISPOT analysis detected similar numbers of functional cells in the PDLNs and spleens of both castrated and sham-treated mice (Fig. 5B). Thus, castration alone did not enhance CD8^{+} T-cell function after immunization, in the presence of the endogenous tumor.

Treg depletion together with castration and immunization did not increase the proportion and number of splenic tetramer-positive CD8^{+} T cells at 2.5 weeks after treatment (Fig. 5A). However, the number of IFN-γ–secreting cells was significantly higher both in the PDLNs and spleen (Fig. 5B). The numbers of tetramer-positive cells (Fig. 5C) and numbers of functional antigen-specific cells (Fig. 5D) remained elevated in the PDLNs and spleens 5 weeks after Treg depletion, showing that enhancement of effector function by Treg depletion is long-lasting.

Treg depletion also enhanced effector responses 5 weeks after castration and immunization of wild-type mice (Supplementary Fig. S3).

Treg expansion in $Pten^{-/-}$ tumor–bearing mice is prevented by *in vivo* IL-2 blockade

Two key cytokines, TGF-β and IL-2, have been shown to play an important role in the generation and expansion of Tregs. To explore the potential mechanism by which Tregs expand after castration in prostate tumor–bearing mice, we measured the serum level of total TGF-β in $Pten^{-/-}$ mice 2.5 weeks after castration or sham castration. Castration did not increase the concentration of serum TGF-β concentration compared with sham-treated animals, although the level was higher in $Pten^{-/-}$ mice than WT nontumor-bearing mice (Supplementary Fig. S4).

IL-2 is the signature cytokine that expands and maintains Tregs (23, 24). Increased IL-2 levels resulting from effector CD8^{+} T cells responding to immunizations have been shown to also amplify Tregs (25). Notably, we found an increased population of CD25^{hi} Treg cells in the PDLNs and spleens of castrated mice, suggesting that cell surface expression of CD25 was increased or a population of CD25^{hi} cells was preferentially expanded (Fig. 6A). We were unable to detect IL-2 in the serum of castrated or sham-treated $Pten^{-/-}$ mice (detection limit, 3.1 pg/mL; data not shown).

To determine whether Treg expansion was prevented by IL-2 blockade, we administered IL-2–neutralizing antibody or isotype control 2 days before castration of $Pten^{-/-}$ mice. We analyzed the percentage and number of Tregs in the PDLNs and spleen 2.5 weeks after castration. Indeed, IL-2 neutralization significantly reduced the percentage and number of

Tregs in the spleen (Fig. 6B). The Treg proportion in the PDLNs was also decreased, but the total number remained the same as the lymph nodes were enlarged. Finally, IL-2 neutralization reduced $CD25^{hi}Foxp3^+$ cells in the spleen and PDLNs (Fig. 6C, $P = 0.07$ for numbers in PDLNs), suggesting that Tregs expanded in response to IL-2 generated after castration.

Discussion

Some studies suggest that androgen is immunosuppressive and can increase the proportion of systemic Tregs and thus dampen or ameliorate autoimmune reactions (4, 5, 26). Other reports showed that effector cell function was increased in prostate tumors early after castration and suggested that hormone blockade or surgical castration were immune stimulatory (17, 27). However, immune augmentation must be short-lived, as castration-resistant disease recurs in many patients.

To separate the effect of androgen ablation from tumor-induced immunosuppression, we evaluated $CD8^+$ T-cell responses to a defined antigen in tumor-free mice. The mutant epitope in UV-8101-RE induces strong $CD8^+$ T-cell responses, can be detected with specific probes, and is not expressed in the prostate. Thus, any responses to this epitope were the result of immunization alone and not complicated by shedding of the antigen from dying prostate cells after castration. The increase in $CD8^+$ T-cell precursor frequency and function at 2.5 weeks after castration and immunization of wild-type mice was abrogated by 5 weeks after castration and paralleled by an increase in systemic Tregs. The correlation between Treg expansion and reduced $CD8^+$ T-cell function was supported by the observation that Treg depletion restored $CD8^+$ T-cell function. Administration of anti-CD25 antibody to deplete Tregs can also deplete $CD8^+$ effector T cells (28, 29). Our results strengthen the notion that the timing of Treg depletion is critical to maintaining $CD8^+$ T-cell function.

The increase in systemic Tregs after castration was also observed in prostate-specific $Pten^{-/-}$ mice. Despite the presence of the endogenous castration-resistant prostate tumor, effector T-cell responses to UV-8101-RE were also generated in $Pten^{-/-}$ mice when Tregs were depleted along with castration. The response was maintained at 5 weeks after castration, showing that effector responses generated after castration in the absence of Tregs are long-lived.

Activation of $CD8^+$ T cells in response to immunization or castration of tumor-bearing mice, which is a form of immunization, induces production of IL-2 by activated cells, which in turn expands the pool of precursors by engaging IL-2R on responder cells (30). CD25, the high-affinity receptor for IL-2, is constitutively expressed by Tregs and is crucial for their development and suppressive function (23, 24). Expansion of Tregs by systemic IL-2 following immunization is observed in a variety of models (31-38), showing a direct link between T-cell activation and amplification of inhibitory mechanisms (25). Our results support these observations, as Treg expansion was not observed in castrated and unimmunized wildtype mice.

In $Pten^{-/-}$ mice, Treg expansion after castration was abrogated by neutralization of IL-2, showing that Treg expansion was driven by IL-2. Serum IL-2 was undetectable by ELISA in castrated or sham-castrated $Pten^{-/-}$ mice and suggested that IL-2 generated by effector cells may be quickly consumed by Tregs.

The critical role of TGF-β in generation and function of $CD4^+CD25^+Foxp3^+$ Tregs has been well established (39-41). Primary prostate cancers produce TGF-β (42-44) and the residual tumor remaining after castration can exert immunosuppressive effects by secreting this cytokine. We detected TGF-β message in the tumors early and late after castration (data not

shown), and similar levels of TGF-β were present in the serum of both intact and castrated $Pten^{-/-}$ mice. The increase in systemic Tregs after castration of $Pten^{-/-}$ mice was accelerated compared with wild-type mice, occurring 2.5 weeks after castration. Tumor-produced TGF-β may synergize with IL-2 generated after castration, resulting in early expansion of Tregs (45).

In summary, we have identified a dual effect of androgen ablation on immune function, which amplified both effector and inhibitory arms of the immune system. This dual function was also implied by a recent study of human prostate cancer samples (46). Therapeutic vaccination for treatment of castration-resistant prostate cancers has a small window of opportunity following androgen ablation that may be widened by the addition of Treg depletion to the regimen.

Supplementary Material

Refer to Web version on PubMed Central for supplementary material.

Acknowledgments

References

1. Jemal A, Siegel R, Xu J, Ward E. Cancer statistics, 2010. CA Cancer J Clin. 2010; 60:277–300. [PubMed: 20610543]

2. Denmeade SR, Isaacs JT. A history of prostate cancer treatment. Nat Rev Cancer. 2002; 2:389–96. [PubMed: 12044015]

3. Rosenberg SA, Yang JC, Restifo NP. Cancer immunotherapy: moving beyond current vaccines. Nat Med. 2004; 10:909–15. [PubMed: 15340416]

4. Fijak M, Schneider E, Klug J, Bhushan S, Hackstein H, Schuler G, et al. Testosterone replacement effectively inhibits the development of experimental autoimmune orchitis in rats: evidence for a direct role of testosterone on regulatory T cell expansion. J Immunol. 2011; 186:5162–72. [PubMed: 21441459]

5. Radojevic K, Arsenovic-Ranin N, Kosec D, Pesic V, Pilipovic I, Perisic M, et al. Neonatal castration affects intrathymic kinetics of T- cell differentiation and the spleen T-cell level. J Endocrinol. 2007; 192:669–82. [PubMed: 17332534]

6. Koh YT, Gray A, Higgins SA, Hubby B, Kast WM. Androgen ablation augments prostate cancer vaccine immunogenicity only when applied after immunization. Prostate. 2009; 69:571–84. [PubMed: 19143030]

7. Arredouani MS, Tseng-Rogenski SS, Hollenbeck BK, Escara-Wilke J, Leander KR, Defeo-Jones D, et al. Androgen ablation augments human HLA2.1-restricted T cell responses to PSA self-antigen in transgenic mice. Prostate. 2010; 70:1002–11. [PubMed: 20209643]

8. Drake CG, Doody AD, Mihalyo MA, Huang CT, Kelleher E, Ravi S, et al. Androgen ablation mitigates tolerance to a prostate/prostate cancer-restricted antigen. Cancer Cell. 2005; 7:239–49. [PubMed: 15766662]

9. Dubey P, Hendrickson RC, Meredith SC, Siegel CT, Shabanowitz J, Skipper JC, et al. The immunodominant antigen of an ultraviolet-induced regressor tumor is generated by a somatic point mutation in the DEAD box helicase p68. J Exp Med. 1997; 185:695–705. [PubMed: 9034148]

10. Akins EJ, Moore ML, Tang S, Willingham MC, Tooze JA, Dubey P. *In situ* vaccination combined with androgen ablation and regulatory T-cell depletion reduces castration-resistant tumor burden in prostate-specific pten knockout mice. Cancer Res. 2010; 70:3473–82. [PubMed: 20406970]

11. Wang S, Gao J, Lei Q, Rozengurt N, Pritchard C, Jiao J, et al. Prostate-specific deletion of the murine Pten tumor suppressor gene leads to metastatic prostate cancer. Cancer Cell. 2003; 4:209–21. [PubMed: 14522255]

12. Cao X, Cai SF, Fehniger TA, Song J, Collins LI, Piwnica-Worms DR, et al. Granzyme B and perforin are important for regulatory T cell-mediated suppression of tumor clearance. Immunity. 2007; 27:635–46. [PubMed: 17919943]

13. Sakaguchi S, Ono M, Setoguchi R, Yagi H, Hori S, Fehervari Z, et al. Foxp3+ CD25+ CD4+ natural regulatory T cells in dominant self-tolerance and autoimmune disease. Immunol Rev. 2006; 212:8–27. [PubMed: 16903903]

14. Murali-Krishna K, Altman JD, Suresh M, Sourdive DJ, Zajac AJ, Miller JD, et al. Counting antigen-specific CD8 T cells: a reevaluation of bystander activation during viral infection. Immunity. 1998; 8:177–87. [PubMed: 9491999]

15. Altman JD, Moss PA, Goulder PJ, Barouch DH, McHeyzer-Williams MG, Bell JI, et al. Phenotypic analysis of antigen-specific T lymphocytes. Science. 1996; 274:94–6. [PubMed: 8810254]

16. Obar JJ, Khanna KM, Lefrancois L. Endogenous naive CD8+ T cell precursor frequency regulates primary and memory responses to infection. Immunity. 2008; 28:859–69. [PubMed: 18499487]

17. Roden AC, Moser MT, Tri SD, Mercader M, Kuntz SM, Dong H, et al. Augmentation of T cell levels and responses induced by androgen deprivation. J Immunol. 2004; 173:6098–108. [PubMed: 15528346]

18. Klages K, Mayer CT, Lahl K, Loddenkemper C, Teng MW, Ngiow SF, et al. Selective depletion of Foxp3+ regulatory T cells improves effective therapeutic vaccination against established melanoma. Cancer Res. 2010; 70:7788–99. [PubMed: 20924102]

19. Nicholaou T, Ebert LM, Davis ID, McArthur GA, Jackson H, Dimopoulos N, et al. Regulatory T-cell-mediated attenuation of T-cell responses to the NY-ESO-1 ISCOMATRIX vaccine in patients with advanced malignant melanoma. Clin Cancer Res. 2009; 15:2166–73. [PubMed: 19276262]

20. Macatangay BJ, Szajnik ME, Whiteside TL, Riddler SA, Rinaldo CR. Regulatory T cell suppression of Gag-specific CD8 T cell polyfunctional response after therapeutic vaccination of HIV-1-infected patients on ART. PLoS One. 2010; 5:e9852. [PubMed: 20352042]

21. Viselli SM, Stanziale S, Shults K, Kovacs WJ, Olsen NJ. Castration alters peripheral immune function in normal male mice. Immunology. 1995; 84:337–42. [PubMed: 7751013]

22. Lapierre P, Beland K, Martin C, Alvarez F Jr, Alvarez F. Forkhead box p3 +regulatory T cell underlies male resistance to experimental type 2 autoimmune hepatitis. Hepatology. 2010; 51:1789–98. [PubMed: 20232291]

23. Fontenot JD, Rasmussen JP, Gavin MA, Rudensky AY. A function for interleukin 2 in Foxp3-expressing regulatory T cells. Nat Immunol. 2005; 6:1142–51. [PubMed: 16227984]

24. Setoguchi R, Hori S, Takahashi T, Sakaguchi S. Homeostatic maintenance of natural Foxp3(+) CD25(+) CD4(+) regulatory T cells by interleukin (IL)-2 and induction of autoimmune disease by IL-2 neutralization. J Exp Med. 2005; 201:723–35. [PubMed: 15753206]

25. McNally A, Hill GR, Sparwasser T, Thomas R, Steptoe RJ. CD4+CD25+ regulatory T cells control CD8+ T-cell effector differentiation by modulating IL-2 homeostasis. Proc Natl Acad Sci U S A. 2011; 108:7529–34. [PubMed: 21502514]

26. Page ST, Plymate SR, Bremner WJ, Matsumoto AM, Hess DL, Lin DW, et al. Effect of medical castration on CD4+ CD25+ T cells, CD8+ T cell IFN-gamma expression, and NK cells: a physiological role for testosterone and/or its metabolites. Am J Physiol Endocrinol Metab. 2006; 290:E856–63. [PubMed: 16352669]

27. Mercader M, Bodner BK, Moser MT, Kwon PS, Park ES, Manecke RG, et al. T cell infiltration of the prostate induced by androgen withdrawal in patients with prostate cancer. Proc Natl Acad Sci U S A. 2001; 98:14565–70. [PubMed: 11734652]

28. Curtin JF, Candolfi M, Fakhouri TM, Liu C, Alden A, Edwards M, et al. Treg depletion inhibits efficacy of cancer immunotherapy: implications for clinical trials. PLoS One. 2008; 3:e1983. [PubMed: 18431473]

29. Quezada SA, Peggs KS, Simpson TR, Shen Y, Littman DR, Allison JP. Limited tumor infiltration by activated T effector cells restricts the therapeutic activity of regulatory T cell depletion against established melanoma. J Exp Med. 2008; 205:2125–38. [PubMed: 18725522]

30. Malek TR, Castro I. Interleukin-2 receptor signaling: at the interface between tolerance and immunity. Immunity. 2010; 33:153–65. [PubMed: 20732639]

31. Weiss L, Letimier FA, Carriere M, Maiella S, Donkova-Petrini V, Targat B, et al. *In vivo* expansion of naive and activated CD4+CD25+FOXP3+ regulatory T cell populations in interleukin-2-treated HIV patients. Proc Natl Acad Sci U S A. 2010; 107:10632–7. [PubMed: 20498045]

32. Berntsen A, Brimnes MK, thor Straten P, Svane IM. Increase of circulating CD4+CD25highFoxp3 +regulatory T cells in patients with metastatic renal cell carcinoma during treatment with dendritic cell vaccination and low-dose interleukin-2. J Immunother. 2010; 33:425–34. [PubMed: 20386464]

33. Brandenburg S, Takahashi T, de la Rosa M, Janke M, Karsten G, Muzzulini T, et al. IL-2 induces *in vivo* suppression by CD4(+)CD25(+) Foxp3(+) regulatory T cells. Eur J Immunol. 2008; 38:1643–53. [PubMed: 18493984]

34. Lemoine FM, Cherai M, Giverne C, Dimitri D, Rosenzwajg M, Trebeden-Negre H, et al. Massive expansion of regulatory T-cells following interleukin 2 treatment during a phase I-II dendritic cell-based immunotherapy of metastatic renal cancer. Int J Oncol. 2009; 35:569–81. [PubMed: 19639177]

35. Liu CL, Ye P, Yen BC, Miao CH. *In vivo* expansion of regulatory T cells with IL-2/IL-2 mAb complexes prevents anti-factor VIII immune responses in hemophilia A mice treated with factor VIII plasmidmediated gene therapy. Mol Ther. 2011; 19:1511–20. [PubMed: 21468007]

36. Scheffold A, Huhn J, Hofer T. Regulation of CD4+CD25+ regulatory T cell activity: it takes (IL-)two to tango. Eur J Immunol. 2005; 35:1336–41. [PubMed: 15827965]

37. Klein L, Khazaie K, von Boehmer H. *In vivo* dynamics of antigenspecific regulatory T cells not predicted from behavior *in vitro*. Proc Natl Acad Sci U S A. 2003; 100:8886–91. [PubMed: 12857946]

38. Barthlott T, Moncrieffe H, Veldhoen M, Atkins CJ, Christensen J, O'Garra A, et al. CD25+ CD4+ T cells compete with naive CD4+ T cells for IL-2 and exploit it for the induction of IL-10 production. Int Immunol. 2005; 17:279–88. [PubMed: 15684039]

39. Chen W, Jin W, Hardegen N, Lei KJ, Li L, Marinos N, et al. Conversion of peripheral CD47+CD25- naive T cells to CD4+CD25+ regulatory T cells by TGF-beta induction of transcription factor Foxp3. J Exp Med. 2003; 198:1875–86. [PubMed: 14676299]

40. Huber S, Schramm C, Lehr HA, Mann A, Schmitt S, Becker C, et al. Cutting edge: TGF-beta signaling is required for the *in vivo* expansion and immunosuppressive capacity of regulatory CD4+CD25+T cells. J Immunol. 2004; 173:6526–31. [PubMed: 15557141]

41. Marie JC, Letterio JJ, Gavin M, Rudensky AY. TGF-beta1 maintains suppressor function and Foxp3 expression in CD4+CD25+ regulatory T cells. J Exp Med. 2005; 201:1061–7. [PubMed: 15809351]

42. Eastham JA, Truong LD, Rogers E, Kattan M, Flanders KC, Scardino PT, et al. Transforming growth factor-beta 1: comparative immunohistochemical localization in human primary and metastatic prostate cancer. Lab Invest. 1995; 73:628–35. [PubMed: 7474936]

43. Jones E, Pu H, Kyprianou N. Targeting TGF-beta in prostate cancer: therapeutic possibilities during tumor progression. Expert Opin Ther Targets. 2009; 13:227–34. [PubMed: 19236240]

44. Steiner MS, Zhou ZZ, Tonb DC, Barrack ER. Expression of transforming growth factor-beta 1 in prostate cancer. Endocrinology. 1994; 135:2240–7. [PubMed: 7956947]

45. Zheng SG, Wang J, Wang P, Gray JD, Horwitz DA. IL-2 is essential for TGF-beta to convert naive CD4+CD25- cells to CD25+Foxp3+ regulatory T cells and for expansion of these cells. J Immunol. 2007; 178:2018–27. [PubMed: 17277105]

46. Sorrentino C, Musiani P, Pompa P, Cipollone G, Di Carlo E. Androgen deprivation boosts prostatic infiltration of cytotoxic and regulatory T lymphocytes and has no effect on disease-free survival in prostate cancer patients. Clin Cancer Res. 2011; 17:1571–81. [PubMed: 21159885]
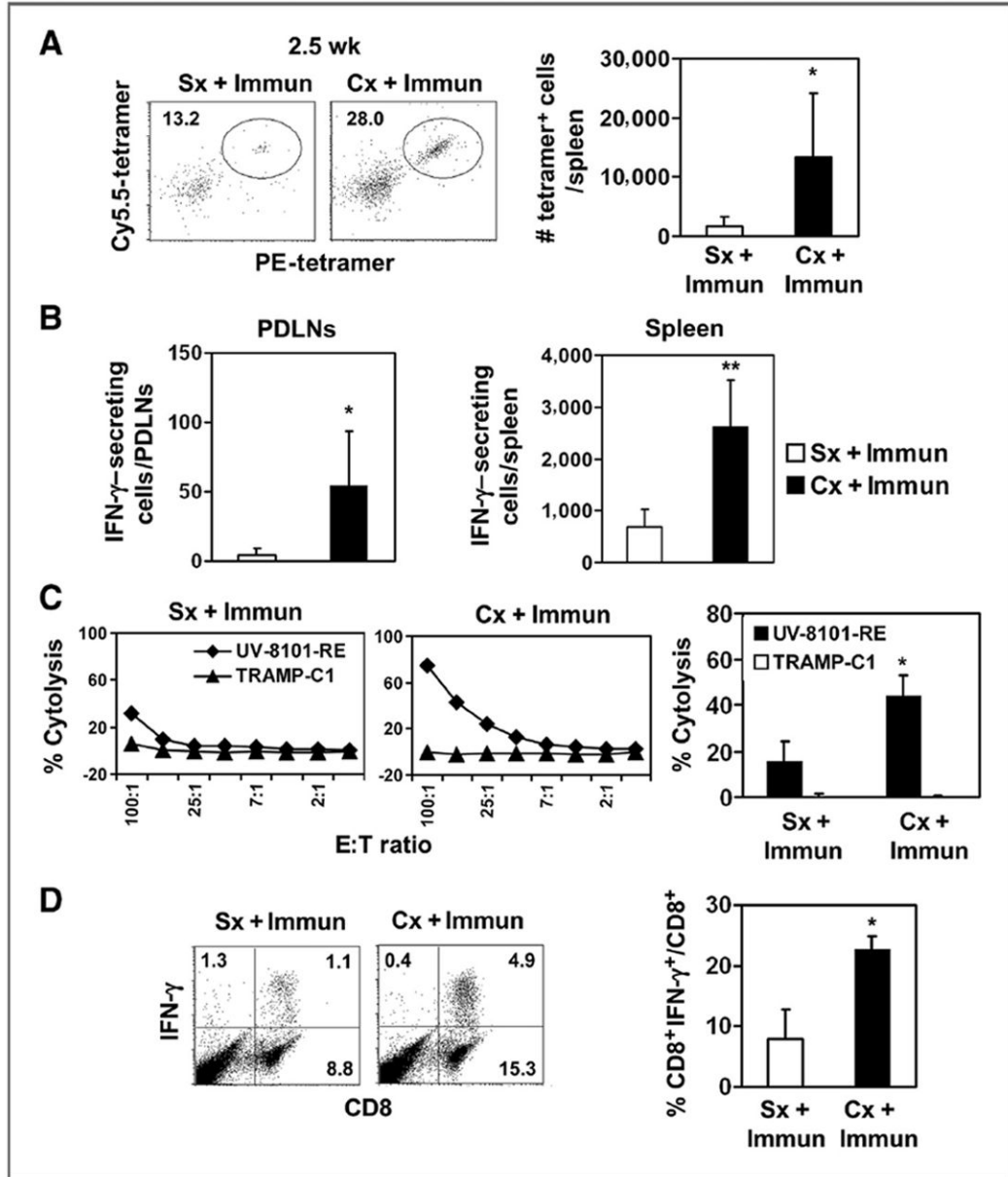
Figure 1.
Enhanced antigen-specific effector responses 2.5 weeks after castration and immunization. A, splenocytes were stained with CD8, CD44, PE-tetramer, and Cy5.5-tetramer. Cells enriched with anti-PE beads were analyzed. The representative dot plot (left) shows PE- and Cy5.5-tetramer double-positive cells gated on the CD8$^+$CD44$^+$ population. The number of tetramer-positive cells was quantified (bar graphs; ■, Cx + Immun; □, Sx + Immun). The experiment was repeated once. B, IFN-γ–secreting cells in response to *ex vivo* UV-8101-RE stimulation were identified using ELISPOT assay with PDLNs (left) and spleen cells (right) from both groups. The average of triplicate wells in 1 representative experiment is shown. C, lytic capacity of MLTC cells, 2.5 weeks after immunization, was determined in a ^{51}Cr release assay. Targets are UV-8101-RE (◆) and TRAMP-C1 (▲). Line graphs show one representative animal from each group and bar graphs show the average of all animals in each group at an effector:target (E:T) ratio of 50:1. D, effector cytokine production was

determined by intracellular cytokine staining of MLTC cells. Flow diagram (left) shows representative samples of CD8$^+$ cells that express IFN-γ after *ex vivo* restimulation. The percentage of CD8$^+$ T cells that express IFN-γ was calculated (right). Data are mean values ± SD. *, $P < 0.05$; **, $P < 0.01$ for Sx + immunization (Immun) versus Cx + immunization. One representative experiment with 3 to 5 animals per group is shown. Each experiment was repeated at least once. Cx, castration; Sx, sham treatment.
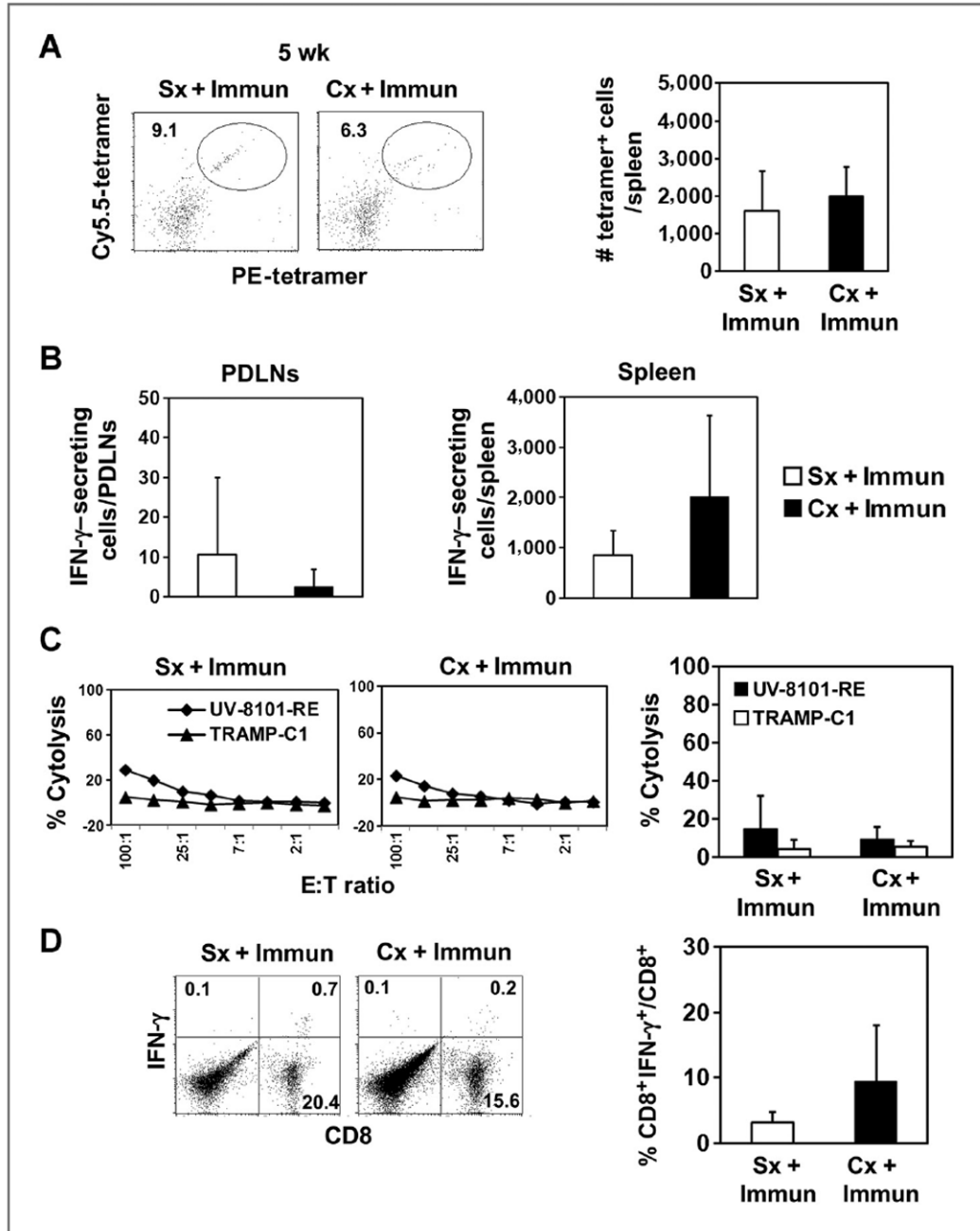
Figure 2.
Enhancement of CD8^{+} effector function by castration was diminished 5 weeks after immunization. A, the representative dot plot (left) shows PE- and Cy5.5-tetramer double-positive cells gated on the CD8^{+}CD44^{+} population as described in Fig. 1. The number of tetramer-positive cells was quantified and represents the average of 5 animals in one experiment (bar graphs; ■, Cx + Immun; □, Sx + Immun). B, IFN-γ–secreting cells in response to *ex vivo* UV-8101-RE stimulation were identified using an ELISPOT assay with PDLNs (left) and spleen cells (right) from both groups. The average of triplicate wells in one representative experiment is shown. C, lytic capacity of MLTC cells cultured for 6 days was determined by ^{51}Cr release assay (◆, UV-8101-RE; ▲, TRAMP-C1). Line graphs

show one representative animal from each group and the bar graph shows the average of all animals in each group at an E:T ratio of 50:1. D, IFN-γ expression by MLTC cells was assessed by an intracellular cytokine staining assay (left). Percentages of IFN-γ–expressing cells gated on CD8$^+$ T cells were calculated (right). Data are presented as mean values $\pm$ SD and one representative experiment of 3 independent experiments with 3 to 5 mice per group is shown. Cx, castration; Immun, immunization; Sx, sham treatment.
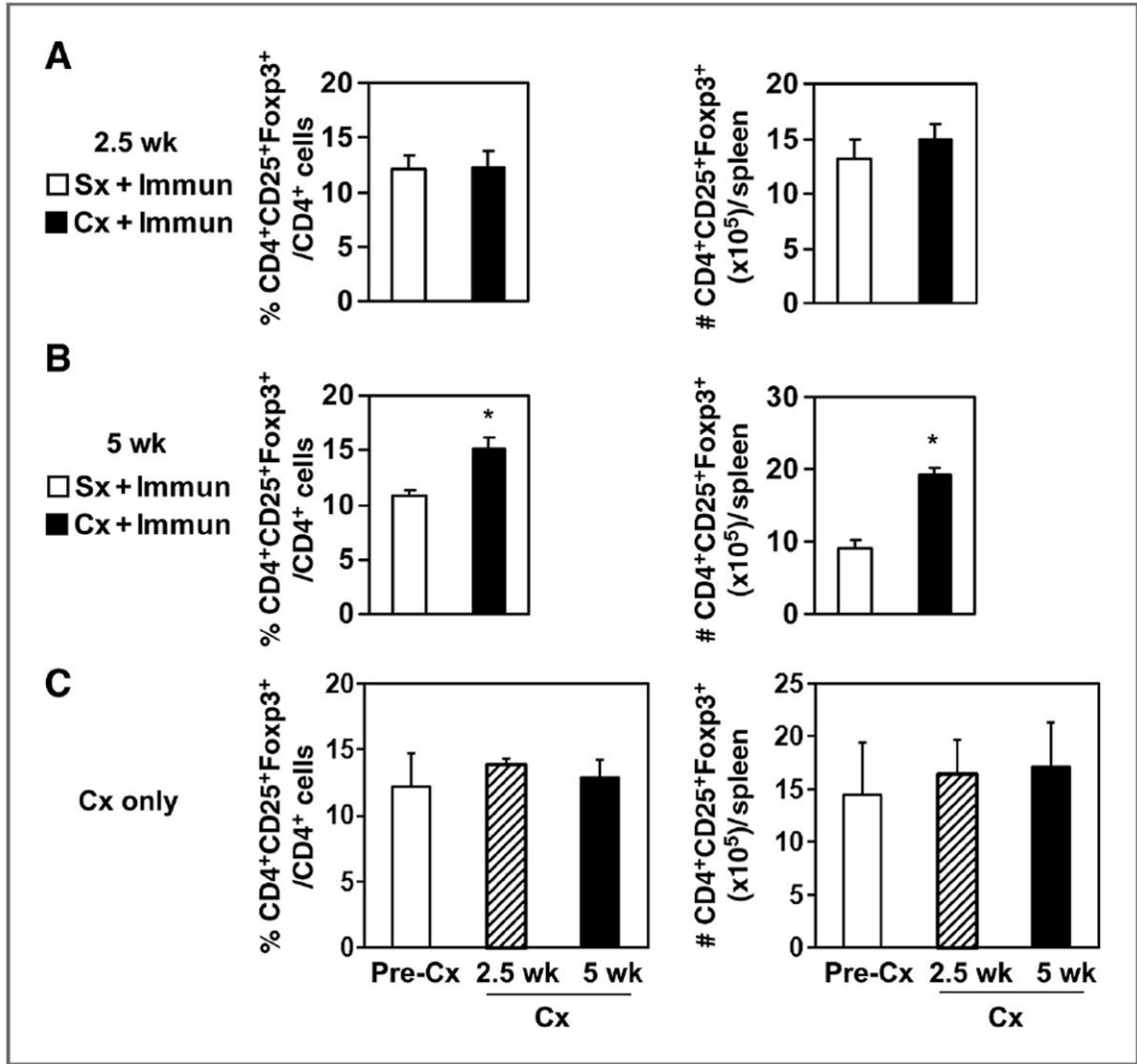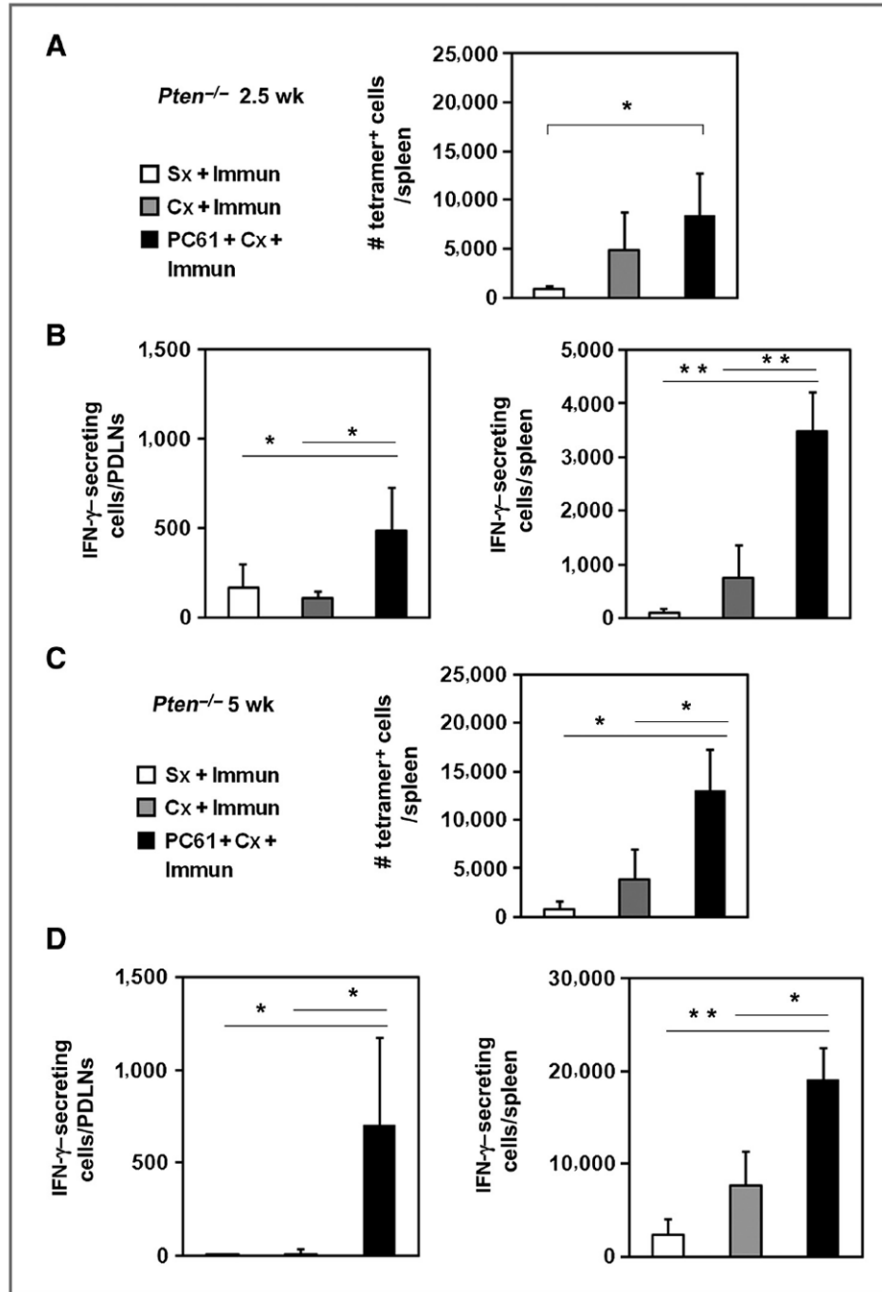
Figure 3.
Castration increased splenic CD4+CD25+Foxp3+ Tregs by 5 weeks after immunization of wild-type mice. Splenocytes from mice isolated at 2.5 weeks (A) or 5 weeks after immunization (B), and castration or sham treatment were analyzed by flow cytometry. The number of CD4+CD25+Foxp3+ cells was calculated by multiplying the percentage of CD4+CD25+Foxp3+ cells times the total number of isolated splenocytes and represents the average of 3 animals in the group. *, $P < 0.01$ versus immunization only group. Data are from one representative experiment of 3 independent repeats. Mice were from the experiments shown in Figs. 1 and 2. C, mice were castrated and analyzed 2.5 weeks or 5 weeks later, as described above. Pooled data of 2 independent experiments are shown with 4 to 5 mice per group in each experiment. Cx, castration; Immun, immunization; Sx, sham treatment.
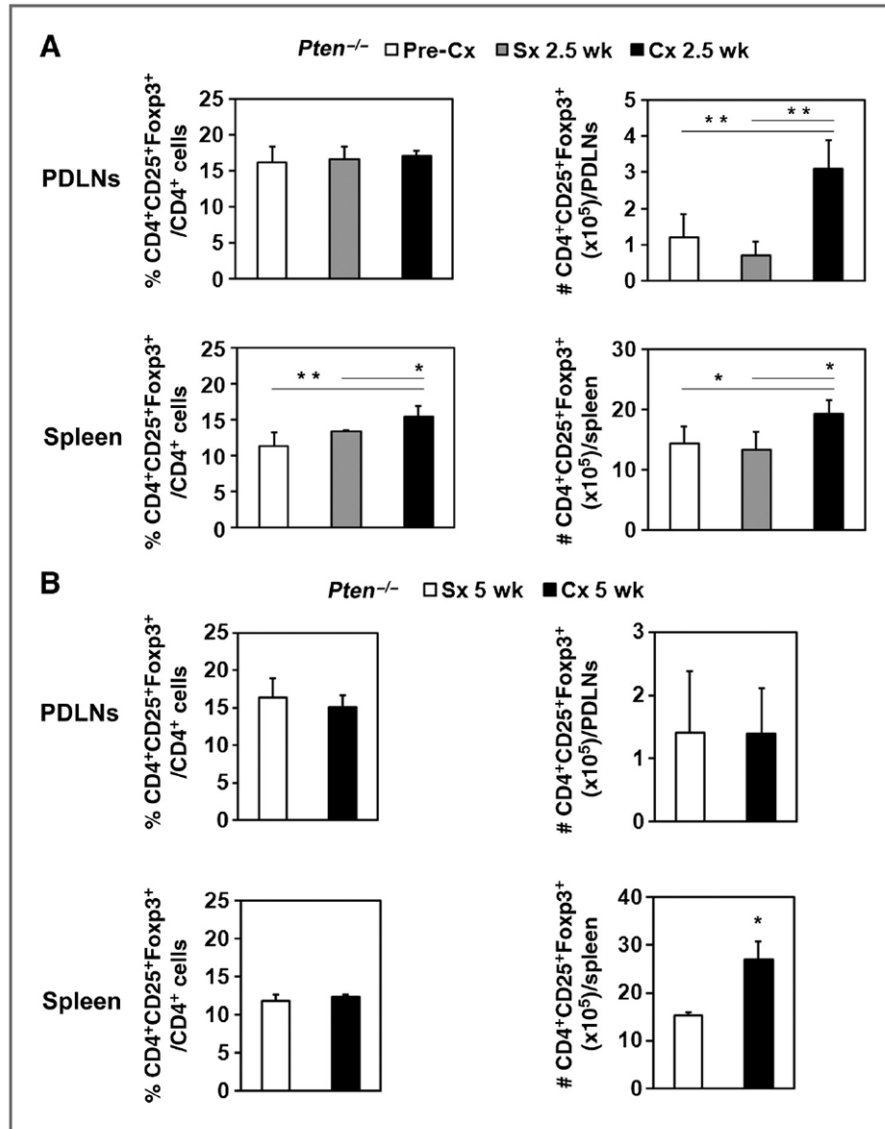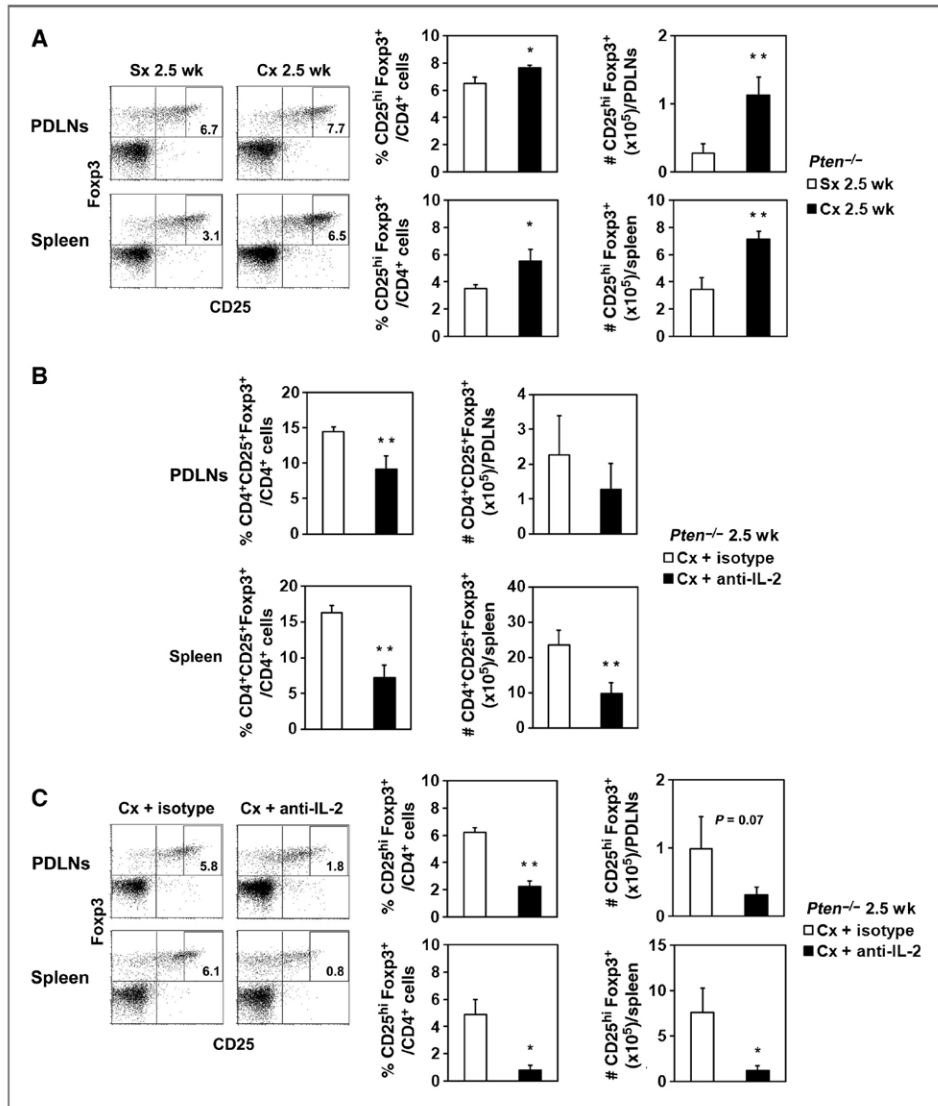
Figure 4.
Castration amplified CD4^{+}CD25^{+}Foxp3^{+} Tregs in the spleen and PDLNs early after castration in prostate tumor–bearing *Pten*^{−/−} mice. A, PDLNs and spleens were harvested from *Pten*^{−/−} mice that were either untreated or 2.5 weeks after castration or sham surgery. Cells were analyzed, and the percentage and number of CD4^{+}CD25^{+}Foxp3^{+} Tregs were quantified as described in Fig. 3. B, PDLN cells and spleens from *Pten*^{−/−} *mice* isolated at 5 weeks after castration or sham surgery were analyzed for the percentage and number of CD4^{+}CD25^{+}FoxP3^{+} Tregs. * $P < 0.05$; **, $P < 0.01$ for Cx group versus Sx group or Pre-Cx group. Pooled data of 2 independent experiments are shown with 3 to 5 mice per group in each experiment. Cx, castration; Sx, sham treatment.

Figure 5.
Effector responses to a tumor antigen were detected only after castration with concomitant Treg depletion in prostate tumor–bearing mice. A, *Pten*^{−/−} mice were analyzed 2.5 weeks after immunization (Immun) and castration (Cx) or sham treatment (Sx). Splenic tetramer-positive cells were enriched by magnetic bead selection followed by flow cytometric analysis. The number of tetramer-positive cells per spleen was calculated (bar graph; □, Sx + Immun; ■, Cx + Immun; ■, Cx + PC61 + Immun). *, $P < 0.05$ for Cx + PC61 + Immun versus Sx + Immun. B, IFN-γ–secreting splenocytes or PDLN cells in response to *ex vivo* UV-8101-RE stimulation were quantified using an ELISPOT assay for all 3 groups. C, the number of tetramer-positive cells per spleen 5 weeks after immunization and castration or

sham surgery of *Pten*$^{-/-}$ mice is shown. D, IFN-γ–secreting cells in spleen or PDLNs following *ex vivo* UV-8101-RE stimulation were quantified using ELISPOT assays for all 3 groups. *, $P < 0.05$; **, $P < 0.001$ for Cx + PC61 + Immun group versus Sx + Immun group or Cx + Immun group. Each group contained 3 to 5 animals, and the experiment was repeated once.

Figure 6.
Treg expansion after castration in *Pten*$^{-/-}$ mice was mediated by IL-2. A, dot plots show CD25$^+$Foxp3$^+$ cells gated on CD4$^+$ cells from PDLNs or spleen of one representative mouse in Sx or Cx groups for 2.5 weeks after castration. The rectangles designate the CD25^{hi} population. The percentage and number of CD4$^+$CD25^{hi}Foxp3$^+$ cells were calculated (bar graphs; ■, Cx 2.5 weeks; □, Sx 2.5 weeks). *, $P < 0.05$; **, $P < 0.01$ for Cx 2.5 weeks compared with Sx 2.5-week group. B, *Pten*$^{-/-}$ mice were injected with anti-IL-2 or isotype control monoclonal antibody 2 days before castration. The proportion and number of CD4$^+$CD25$^+$Foxp3$^+$ were quantified in PDLNs and spleens 2.5 weeks after treatment (bar graphs; ■, Cx + anti-IL-2; □, Cx + isotype). **, $P < 0.01$ for Cx + anti-IL-2 compared with Cx + isotype group. Each group contained 3 mice, and the experiment was repeated once. C, representative dot plots of CD25$^+$Foxp3$^+$ staining gated on CD4$^+$ cells from PDLNs or spleens are shown for one mouse in the Cx + anti-IL-2 or Cx + isotype group. The percentage and number of CD4$^+$CD25^{hi}Foxp3$^+$ cells were quantified (bar graphs; ■, Cx + anti-IL-2; □, Cx + isotype). Mice were from the same experiment as in B. *, $P < 0.05$; **, P

< 0.001 for Cx + anti-IL-2 compared with Cx + isotype group. Cx, castration; Sx, sham treatment.